

DOI: 10.1002/ejic.201200069

## 2,2'-Diborylazobenzenes with Double N–B Coordination: Control of Fluorescent Properties by Substituents and Redox Reactions

Naokazu Kano,<sup>\*[a]</sup> Akiko Furuta,<sup>[a]</sup> Tetsuya Kambe,<sup>[a]</sup> Junro Yoshino,<sup>[a]</sup> Yusuke Shibata,<sup>[a]</sup> Takayuki Kawashima,<sup>\*[a][‡]</sup> Naomi Mizorogi,<sup>[b]</sup> and Shigeru Nagase<sup>[b]</sup>

**Keywords:** Boron / Fluorescence / Redox chemistry / Radical ions

2,2'-Bis[bis(pentafluorophenyl)boryl]azobenzenes were synthesized. X-ray crystallographic analysis exhibits a planar core structure of the azobenzene moiety, double intramolecular N–B coordination, and two tetracoordinate boron atoms. The 2,2'-diborylazobenzenes show fluorescence emission with orange and red colors upon irradiation. The double N–B coordination causes redshifts in both the absorption and emission maxima and a decrease in the Stokes shifts relative to those of the 2-borylazobenzene derivative. On the basis of the density functional theory calculations of the molecular

orbitals of 2,2'-diborylazobenzene, the  $\pi^*$  orbital (LUMO) was found at a much lower energy level (–4.67 eV) than that in 2-borylazobenzene (–3.70 eV). A reversible reduction wave was observed at a low reduction potential in the cyclic voltammograms of the 2,2'-diborylazobenzenes. Single-electron reduction of one of the 2,2'-diborylazobenzenes generates an azobenzene radical anion, which was confirmed by an active ESR signal. The fluorescence was quenched by the reduction and recovered by air oxidation in this azobenzene.

### Introduction

Some popular organic dyes can be used as fluorescent dyes, which are important for light-emitting devices, fluorescent probes of living tissues, and molecular detection.<sup>[1]</sup> Azo dyes are the most frequently used dyes and popular chromophores;<sup>[2]</sup> however, azobenzenes, the chromogen of the azo dyes, usually do not fluoresce,<sup>[3]</sup> except for a few faintly fluorescent examples such as *ortho*-metallated azobenzenes<sup>[4]</sup> and self-assembled aggregates of azobenzene derivatives.<sup>[5]</sup> Intramolecular coordination from nitrogen to boron, as seen in BODIPY,<sup>[6]</sup> conveniently changes nonfluorescent heteroaromatics to fluorescent molecules.<sup>[7]</sup> Indeed, we synthesized green-fluorescent 2-[bis(pentafluorophenyl)boryl]azobenzene [(*E*)-**1a**] (Figure 1), in which the intramolecular N–B coordination effectively restricts conformational freedom of one benzene ring and changes the HOMO and LUMO energy levels.<sup>[8]</sup> Fluorescence emission of other colors and control of the emission by redox reactions are desirable for application to functional materials such as organic light-emitting diodes. Doubling the N–B

coordination can achieve the task by extension of the  $\pi$ -conjugation and perturbation of the molecular orbitals (Figure 1).<sup>[9]</sup> We report here the synthesis of 2,2'-diborylazobenzenes that have double intramolecular N–B coordination and control of their fluorescent properties.

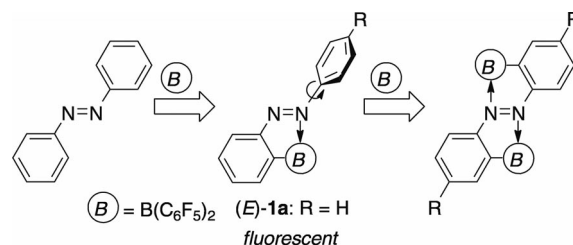


Figure 1. Molecular design for conformational fixation of an azobenzene.

### Results and Discussion

Successive reactions of (*E*)-2,2'-diidoazobenzenes (*E*)-**2a–d** with *n*BuLi and (C<sub>6</sub>F<sub>5</sub>)<sub>2</sub>BOEt gave 2,2'-diborylazobenzenes (*E*)-**3a–d** as air-stable solids (Scheme 1). Their <sup>11</sup>B NMR spectra in CDCl<sub>3</sub> [ $\delta$  = –2.9 to –1.6 ppm] show that they have tetracoordinate boron atoms.<sup>[8a]</sup>

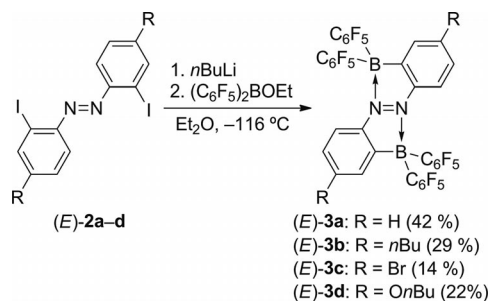
X-ray crystallographic analysis of (*E*)-**3a** reveals its almost C<sub>2</sub>-symmetrical structure and the double intramolecular N–B coordination [N–B: 1.634(3), 1.635(3) Å] (Figure 2).<sup>[10]</sup> The N1–N2 bond length [1.292(3) Å] is within the range of a double bond. The torsion angles around the azo moiety [N1–N2–C6–C5: 176.5(2)°, N2–N1–C24–C23:

[a] Department of Chemistry, Graduate School of Science, The University of Tokyo, 7-3-1 Hongo, Bunkyo-ku, Tokyo 113-0033, Japan  
E-mail: kano@chem.s.u-tokyo.ac.jp

[b] Department of Theoretical and Computational Molecular Science, Institute for Molecular Science, Myodaiji, Okazaki 444-8585, Japan

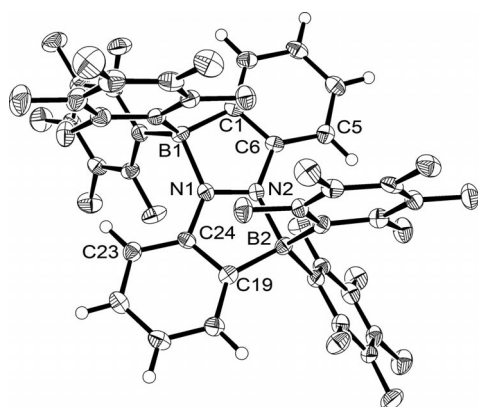
[‡] Present address: Faculty of Science, Gakushuin University, 1-5-1 Mejiro, Toshima-ku, Tokyo, 171-8588, Japan  
E-mail: Takayuki.Kawashima@gakushuin.ac.jp

Supporting information for this article is available on the WWW under <http://dx.doi.org/10.1002/ejic.201200069>.

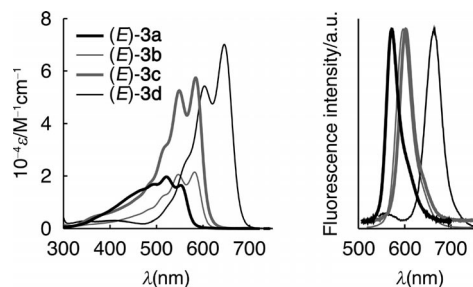


Scheme 1.

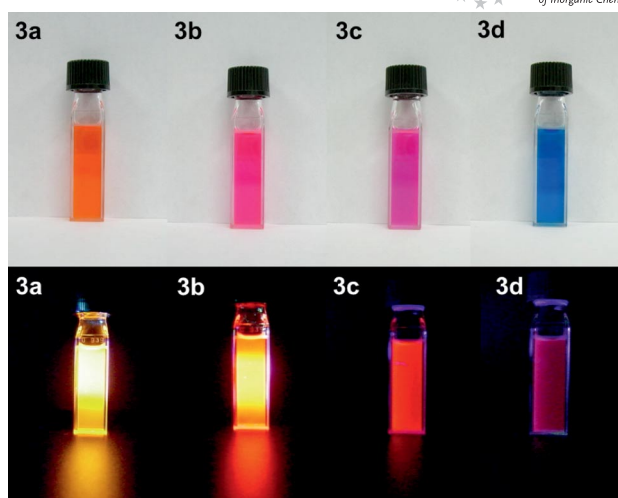
175.3(2)°] show that its coplanarity is greater than that in (*E*)-**1a**.<sup>[8a,8c]</sup> This structural motif, where two main group elements bridge the azo group to form fused five-membered rings, is quite rare.<sup>[9,11]</sup>

Figure 2. ORTEP drawing of (*E*)-**3a** (thermal ellipsoid plot with 50% probability).

Hexane solutions of (*E*)-**3a-d** show orange, pink, purple, and blue colors, respectively, with longer absorption maxima,  $\lambda_{\text{abs}}$ , in the UV/Vis spectra than those for PhN=NPh [(*E*)-**4**] and (*E*)-**1a** (Figures 3 and 4, Table 1). The large redshifts are caused by effective  $\pi$ -conjugation, which reflects good coplanarity.

Figure 3. UV/Vis absorption and fluorescence spectra of (*E*)-**3a-d** in hexane.

Irradiation of (*E*)-**3a-d** in hexane causes orange or red fluorescence emission, unlike the nonfluorescent behavior of most normal azobenzene derivatives (Figure 4). In the fluorescence spectra of (*E*)-**3a-d** (excitation at 500 nm), the emission maxima  $\lambda_{\text{FL}}$  are between 572 and 663 nm, much longer than that of (*E*)-**1a** (Figure 3).<sup>[8a]</sup> Moreover, their

Figure 4. Photographs of (*E*)-**3a-d** in hexane under room light (top) and UV light (bottom).Table 1. Optical data for (*E*)-**3a-d** and related azobenzene derivatives in hexane.

	R	$\lambda_{\text{abs}}$ (nm)	log $\epsilon$	$\lambda_{\text{FL}}$ (nm)	$\Phi_{\text{F}}$	Stokes shift (cm <sup>-1</sup> )
( <i>E</i> )- <b>1a</b> <sup>[a]</sup>	H	386	4.28	503	0.20	6000
( <i>E</i> )- <b>4</b> <sup>[a]</sup>	–	315	4.35	–	–	–
( <i>E</i> )- <b>3a</b>	H	521, 552	4.30, 4.20	572	0.26	630
( <i>E</i> )- <b>3b</b>	<i>n</i> Bu	547, 582	4.41, 4.33	597	0.73	430
( <i>E</i> )- <b>3c</b>	Br	549, 584	4.72, 4.76	602	0.39	510
( <i>E</i> )- <b>3d</b>	<i>On</i> Bu	603, 646	4.74, 4.85	663	0.62	400

[a] Ref.<sup>[8c]</sup>

Stokes shifts (400–630 cm<sup>-1</sup>) are much smaller than that of (*E*)-**1a** (6000 cm<sup>-1</sup>), which reflects their rigid conformation. Their fluorescence quantum yields,  $\Phi_{\text{F}}$ , range from 0.26 to 0.73 (Table 1), which are much higher than the value of  $2.53 \times 10^{-5}$  for (*E*)-**4**.<sup>[12]</sup> Considering that (*E*)-**3a** is formed by additional N–B bond formation between (*E*)-**1a** and the boryl group (a Lewis acid moiety), the fluorescence emission of (*E*)-**3a** remarkably contrasts the fluorescence quenching of (*E*)-**1a** by N–H bond formation upon addition of a Brønsted acid.<sup>[8b]</sup> Moreover, in (*E*)-**3a-d**, all alkyl, bromo, and alkoxy groups at the 4- and 4'-positions cause both redshifts and an increase in  $\Phi_{\text{F}}$  values.

The molecular orbitals of (*E*)-**3a**, studied by density functional theory (DFT) calculations at the B3PW91/6-31+G(d) level of theory, were compared with those of (*E*)-**1a** and (*E*)-**4**.<sup>[8a,8c,13]</sup> The  $\pi$  orbital, which is the HOMO (energy level: -6.45 eV) in (*E*)-**4**, is stabilized considerably by N–B coordination, which corresponds to HOMO-19 (-10.7 eV) in (*E*)-**3a** and HOMO-8 (-8.9 eV) in (*E*)-**1a**. In addition, the  $\pi^*$  orbital (LUMO) in (*E*)-**3a** is found at a lower energy level (-4.67 eV) than those in (*E*)-**1a** (-3.70 eV) and (*E*)-**4** (-2.55 eV).

The electrochemical properties of (*E*)-**3a,b** were studied by cyclic voltammetry. The cyclic voltammogram of (*E*)-**3a** exhibits a reversible reduction wave at  $E_{1/2} = -0.13$  V ( $E_{\text{pc}} = -0.17$  V,  $E_{\text{pa}} = -0.09$  V) vs. Ag/Ag<sup>+</sup> in CH<sub>2</sub>Cl<sub>2</sub>, while (*E*)-

**4** shows an irreversible reduction wave ( $E_{pc} = -1.07$  V). In addition, (*E*)-**3b** exhibits a similar reversible reduction wave [(*E*)-**3b**:  $E_{1/2} = -0.28$  V]. In accordance with the calculated low LUMO level, the reduction potentials suggest that (*E*)-**3a,b** can be reduced more easily than (*E*)-**4** and (*E*)-**1a** ( $E_{1/2} = -0.81$  V). Hence, (*E*)-**3b**, which fluoresces most brightly among (*E*)-**3a–d**, was reduced chemically by treatment with decamethylcobaltocene (1 equiv.) in THF to generate an azobenzene radical anion, an intermediate in the redox interconversion between an azobenzene and a hydrazobenzene.<sup>[14]</sup> Formation of the azobenzene radical anion **5b** was confirmed by the color change from red to blue [**5b**:  $\lambda_{abs}$  (THF) = 613 nm] and an active ESR signal (Scheme 2, Figure 5). The ESR spectra of **5b** in THF at both 4.2 and 100 K show a broad signal with a *g* value of 2.0037 without a resolved hyperfine splitting (peak-to-peak width 32 G). Such broadening of the signal without any hyperfine coupling was also found in the ESR spectra of 2-(aryloxy)pyridine radical anions and arylazoimine radical anions with nitrogen–metal coordination.<sup>[15]</sup> In these literature cases, the <sup>14</sup>N hyperfine splitting is small in these  $\pi$ -radicals, and it is difficult to resolve it in the ESR spectrum because of dominant anisotropic contributions. The DFT calculations at the UB3PW91/6-31+G(d) level show that the SOMO of **5b** has a large azo- $\pi^*$  character (see Supporting Information). The broadening of the ESR spectrum can be explained similarly to that in the literature. Exposure of a THF solution of **5b** to air leads to rapid oxidation, to recover (*E*)-**3b**. The apparent color change is demonstrated by a conspicuous difference in the absorption spectra [(*E*)-**3b**:  $\lambda_{abs}$  (THF) = 558, 592 nm]. Moreover, **5b** does not fluoresce. The absorption and fluorescence properties of (*E*)-**3b** can be switched reversibly by single-electron re-

duction and oxidation reactions. Control of the fluorescent properties of an azobenzene by doubling the N–B coordination and the redox reactions is significant for further application.

## Conclusions

We synthesized four 2,2'-diborylazobenzenes with a double intramolecular N–B coordination, which results in the planar structure of the azobenzene core. The azobenzenes fluoresce with orange and red colors with fluorescence quantum yields ( $\Phi_F$ ) ranging from 0.26 to 0.73. These fluorescence colors and small Stokes shifts are in contrast to those of 2-borylazobenzene derivatives. The LUMO of the 2,2'-diborylazobenzene is the  $\pi^*$  orbital of the azobenzene moiety and is found at a much lower energy level than that in the 2-borylazobenzene. The single-electron reduction of one of the 2,2'-diborylazobenzenes generated an azobenzene radical anion, which does not fluoresce at all, and air oxidation recovers its fluorescence emission. The reversible changes in both the absorption and emission colors by electrochemical processes may open perspectives for its use in optoelectronic devices.

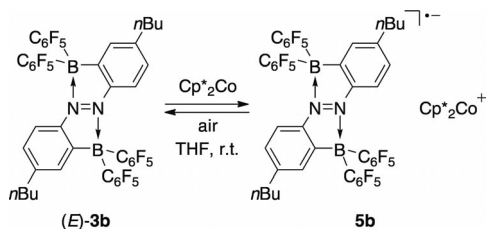
## Experimental Section

*n*BuLi (1.5 M in hexane, 2.1 mL, 3.15 mmol) and an Et<sub>2</sub>O solution (10 mL) of ethoxy[bis(pentafluorophenyl)]borane (1.99 mL, 3.18 mmol) were successively added to 2,2'-diiodoazobenzene (600 mg, 1.38 mmol) in Et<sub>2</sub>O (300 mL) at  $-116$  °C. After gradual warming of the mixture to room temperature, evaporation of solvents, separation by silica gel column chromatography, and recrystallization from hexane gave (*E*)-**3a** (0.50 g, 42%). Red solid. M.p.  $>400$  °C. <sup>1</sup>H NMR (400 MHz, CDCl<sub>3</sub>):  $\delta$  = 7.47 (t, <sup>3</sup>*J* = 7.7 Hz, 2 H), 7.63 (t, <sup>3</sup>*J* = 7.7 Hz, 2 H), 7.79 (d, <sup>3</sup>*J* = 7.7 Hz, 2 H), 7.93 (d, <sup>3</sup>*J* = 7.7 Hz, 2 H) ppm. <sup>11</sup>B NMR (128 MHz, CDCl<sub>3</sub>):  $\delta$  =  $-1.6$  (line width  $h_{1/2}$  = 783 Hz) ppm. <sup>13</sup>C{<sup>1</sup>H} NMR (100 MHz, CDCl<sub>3</sub>):  $\delta$  = 111.3 (br. s), 122.4 (s), 130.0 (s), 130.4 (s), 136.7 (s), 137.4 (dm, <sup>1</sup>*J*<sub>CF</sub> = 254.9 Hz), 138.7 (dm, <sup>1</sup>*J*<sub>CF</sub> = 245.4 Hz), 147.1 (s), 147.7 (dm, <sup>1</sup>*J*<sub>CF</sub> = 241.7 Hz), 157.3 (br. s) ppm. <sup>19</sup>F NMR (376 MHz, CDCl<sub>3</sub>):  $\delta$  =  $-162.63$  (t, <sup>3</sup>*J* = 18.4 Hz, 8 F),  $-155.13$  (t, <sup>3</sup>*J* = 18.4 Hz, 4 F),  $-131.65$  (t, <sup>3</sup>*J* = 18.4 Hz, 8 F) ppm. MS (FAB): *m/z* = 898 [M<sup>+</sup>]. C<sub>36</sub>H<sub>8</sub>B<sub>2</sub>F<sub>20</sub>N<sub>2</sub> (870.05): calcd. C 49.70, H 0.93, N 3.22; found C 49.63, H 1.19, N 3.12.

**Supporting Information** (see footnote on the first page of this article): Synthetic procedures, spectroscopic data, cyclic voltammograms, UV/Vis spectra, ESR measurements, and DFT calculations are presented.

## Acknowledgments

We thank Tosoh Finechem Corp. for the gift of butyllithium. This work was supported by Grants-in-Aid for the GCOE Program and for Scientific Researches (No. 22108508, 22685005, 08J06720) from MEXT and JSPS. N. K. thanks JGC-S Scholarship Foundation, Shorai Foundation for Science and Technology, and Mitsubishi Chemical Corp. Fund for research grants.



Scheme 2. Formation of azobenzene radical anion **5b** from (*E*)-**3b**.

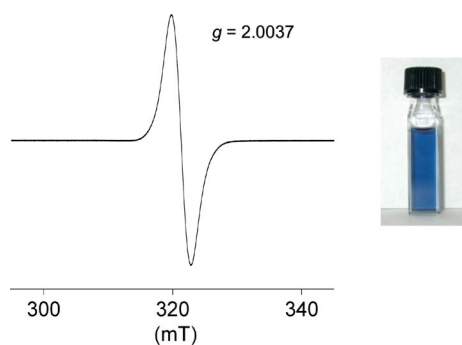


Figure 5. An ESR spectrum of **5b** at 4.2 K (left) and a photograph of **5b** in THF (right).

- [1] a) B. Valeur, *Molecular Fluorescence: Principles and Applications*, Wiley-VCH, New York, **2001**; b) A. P. Demchenko, *Introduction to Fluorescence Sensing*, Springer, **2009**.
- [2] A. Stolz, *Appl. Microbiol. Biotechnol.* **2001**, *56*, 69–80.
- [3] H. Rau, *Angew. Chem.* **1973**, *85*, 248–258; *Angew. Chem. Int. Ed. Engl.* **1973**, *12*, 224–235.
- [4] a) Y. Wakatsuki, H. Yamazaki, P. A. Grutsch, M. Santhanam, C. Kotal, *J. Am. Chem. Soc.* **1985**, *107*, 8153–8159; b) M. Ghedini, D. Pucci, G. Calogero, F. Barigelletti, *Chem. Phys. Lett.* **1997**, *267*, 341–344; c) M. Ghedini, D. Pucci, A. Crispini, I. Aiello, F. Barigelletti, A. Gessi, O. Francescangeli, *Appl. Organomet. Chem.* **1999**, *13*, 565–581; d) I. Aiello, M. Ghedini, M. La Deda, *J. Lumin.* **2002**, *96*, 249–259.
- [5] a) M. Shimomura, T. Kunitake, *J. Am. Chem. Soc.* **1987**, *109*, 5175–5183; b) M. Han, M. Hara, *J. Am. Chem. Soc.* **2005**, *127*, 10951–10955; c) M. R. Han, M. Hara, *New J. Chem.* **2006**, *30*, 223–227.
- [6] a) A. Loudet, K. Burgess, *Chem. Rev.* **2007**, *107*, 4891–4932; b) G. Ulrich, R. Ziessel, A. Harriman, *Angew. Chem.* **2008**, *120*, 1202–1219; *Angew. Chem. Int. Ed.* **2008**, *47*, 1184–1201.
- [7] a) A. Wakamiya, T. Taniguchi, S. Yamaguchi, *Angew. Chem.* **2006**, *118*, 3242–3245; *Angew. Chem. Int. Ed.* **2006**, *45*, 3170–3173; b) S.-F. Liu, Q. Wu, H. L. Schmider, H. Aziz, N.-X. Hu, Z. Popovic, S. Wang, *J. Am. Chem. Soc.* **2000**, *122*, 3671–3678.
- [8] a) J. Yoshino, N. Kano, T. Kawashima, *Chem. Commun.* **2007**, 559–561; b) J. Yoshino, N. Kano, T. Kawashima, *Chem. Lett.* **2008**, *37*, 960–961; c) J. Yoshino, A. Furuta, T. Kambe, H. Itoi, N. Kano, T. Kawashima, Y. Ito, M. Asashima, *Chem. Eur. J.* **2010**, *16*, 5026–5035; d) H. Itoi, T. Kambe, N. Kano, T. Kawashima, *Inorg. Chim. Acta* **2012**, *381*, 117–123.
- [9] M. Yamamura, N. Kano, T. Kawashima, T. Matsumoto, J. Harada, K. Ogawa, *J. Org. Chem.* **2008**, *73*, 8244–8249.
- [10] (*E*)-**3a**: C<sub>36</sub>H<sub>8</sub>B<sub>2</sub>F<sub>20</sub>N<sub>2</sub>, *M<sub>r</sub>* = 870.06, monoclinic, *P*2<sub>1</sub>/*c*, *a* = 11.242(4), *b* = 16.568(5), *c* = 17.165(6) Å, β = 97.7771(16)°, *V* = 3167.5(18) Å<sup>3</sup>, *Z* = 4, ρ<sub>calcd.</sub> = 1.825 Mg/m<sup>3</sup>, μ = 0.190 mm<sup>-1</sup>, *T* = 120(2) K, 18546 measured and 5525 independent reflections, 541 parameters, GOF = 1.106, *R*1[*I* > 2σ(*I*)] = 0.0421, *wR*2 (all data) = 0.1153. CCDC-851780 contains the supplementary crystallographic data for this paper. These data can be obtained free of charge from The Cambridge Crystallographic Data Centre via www.ccdc.cam.ac.uk/data\_request/cif.
- [11] P. Mallikaratchym, R. E. Norman, F. R. Fronczek, T. Junk, *Acta Crystallogr., Sect. E: Struct. Rep. Online* **2005**, *61*, m1370–m1372.
- [12] T. Fujino, S. Yu. Arzhantsev, T. Tahara, *J. Phys. Chem. A* **2001**, *105*, 8123–8129.
- [13] M. J. Frisch, G. W. Trucks, H. B. Schlegel, G. E. Scuseria, M. A. Robb, J. R. Cheeseman, J. A. Montgomery Jr., T. Vreven, K. N. Kudin, J. C. Burant, J. M. Millam, S. S. Iyengar, J. Tomasi, V. Barone, B. Mennucci, M. Cossi, G. Scalmani, N. Rega, G. A. Petersson, H. Nakatsuji, M. Hada, M. Ehara, K. Toyota, R. Fukuda, J. Hasegawa, M. Ishida, T. Nakajima, Y. Honda, O. Kitao, H. Nakai, M. Klene, X. Li, J. E. Knox, H. P. Hratchian, J. B. Cross, C. Adamo, J. Jaramillo, R. Gomperts, R. E. Stratmann, O. Yazyev, A. J. Austin, R. Cammi, C. Pomelli, J. W. Ochterski, P. Y. Ayala, K. Morokuma, G. A. Voth, P. Salvador, J. J. Dannenberg, V. G. Zakrzewski, S. Dapprich, A. D. Daniels, M. C. Strain, O. Farkas, D. K. Malick, A. D. Rabuck, K. Raghavachari, J. B. Foresman, J. V. Ortiz, Q. Cui, A. G. Baboul, S. Clifford, J. Cioslowski, B. B. Stefanov, G. Liu, A. Liashenko, P. Piskorz, I. Komaromi, R. L. Martin, D. J. Fox, T. Keith, M. A. Al-Laham, C. Y. Peng, A. Nanayakkara, M. Challacombe, P. M. W. Gill, B. Johnson, W. Chen, M. W. Wong, C. Gonzalez, J. A. Pople, *Gaussian 03, Revision C.01*, Gaussian, Inc., Wallingford, CT, **2004**.
- [14] S. Cheng, M. D. Hawley, *J. Org. Chem.* **1985**, *50*, 3388–3392.
- [15] a) C. K. Pal, S. Chattopadhyay, C. Sinha, A. Chakravorty, *Inorg. Chem.* **1994**, *33*, 6140–6147; b) C. K. Pal, S. Chattopadhyay, C. Sinha, A. Chakravorty, *Inorg. Chem.* **1996**, *35*, 2442–2447; c) M. Shivakumar, K. Pramanik, P. Ghosh, A. Chakravorty, *Inorg. Chem.* **1998**, *37*, 5968–5969.

Received: January 23, 2012

Published Online: February 21, 2012